



**HAL**  
open science

# The effect of thermal cycling on the high-temperature creep behaviour of a single crystal nickel-based superalloy

Aymeric Raffaitin, Daniel Monceau, Fabrice Crabos, Eric Andrieu

► **To cite this version:**

Aymeric Raffaitin, Daniel Monceau, Fabrice Crabos, Eric Andrieu. The effect of thermal cycling on the high-temperature creep behaviour of a single crystal nickel-based superalloy. *Scripta Materialia*, 2007, 56 (4), pp.277-280. 10.1016/j.scriptamat.2006.10.026 . hal-03593753

**HAL Id: hal-03593753**

**<https://hal.science/hal-03593753v1>**

Submitted on 2 Mar 2022

**HAL** is a multi-disciplinary open access archive for the deposit and dissemination of scientific research documents, whether they are published or not. The documents may come from teaching and research institutions in France or abroad, or from public or private research centers.

L'archive ouverte pluridisciplinaire **HAL**, est destinée au dépôt et à la diffusion de documents scientifiques de niveau recherche, publiés ou non, émanant des établissements d'enseignement et de recherche français ou étrangers, des laboratoires publics ou privés.

# The effect of thermal cycling on the high-temperature creep behaviour of a single crystal nickel-based superalloy

Aymeric Raffaitin, Daniel Monceau, Fabrice Crabos and Eric Andrieu

CIRIMAT UMR 5085, ENSIACET-INPT, 31077 Toulouse Cedex 4, France  
TURBOMECA, 64511 Bordes, France

Isothermal and thermal cycling creep behaviours of a single crystal nickel-based superalloy have been studied by means of tensile tests at 1150 °C and 80 MPa. We have demonstrated that thermal cycling creep rates are faster than isothermal creep rates and that lifetimes at high temperatures are shorter for creep tests under thermal cycling conditions. Furthermore, it is shown that thermal cycling creep lifetime increases as the thermal cycle frequency decreases.

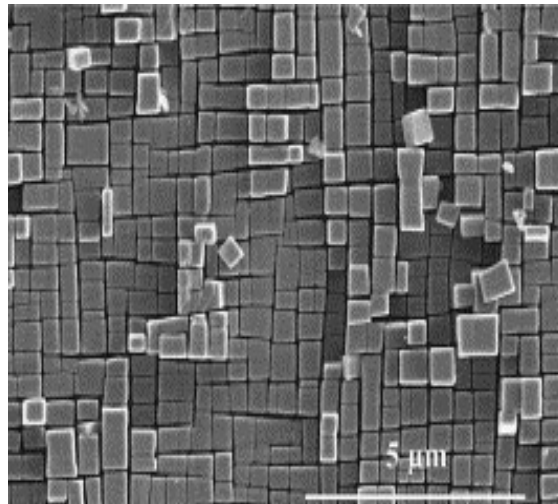
**Keywords:** Nickel-based superalloy; Thermal cycling creep; High temperature creep; Creep rate

Single crystal turbine blades and vanes made of nickel-based superalloys are used in the most advanced gas turbine engines for aircraft and helicopters [1]. These alloys consist of precipitates of an ordered  $L1_2$   $Ni_3Al$ -based phase ( $\gamma'$ ) in a disordered face-centred cubic (fcc) austenitic  $\gamma$  matrix. They offer significant strength and good high-temperature properties, allowing long-term operation of the blade material at temperatures up to about 1100 °C. However, few tensile creep tests results are available at temperatures higher than 1050 °C; data are, instead, generally obtained with isothermal creep tests, which are not representative of the thermal history of a turbine blade. At high temperature, the dissolution of the coherent  $\gamma'$  precipitates and their subsequent reprecipitation on cooling can affect the mechanical behaviour of the alloy and the creep lifetime.

The present study demonstrates the effect of thermal cycling on the creep properties of a single crystal Ni-based superalloy. In order to achieve this objective, the alloy was subjected to thermal cycling under a constant stress.

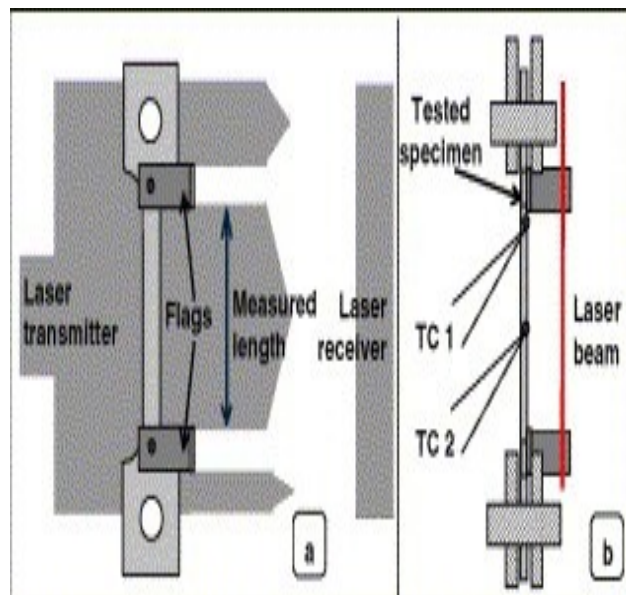
Thin-wall (1 mm thick) creep specimens were barrier machined by spark erosion from a rod specimen made of single crystal nickel-based superalloy MC2 [2]. The nominal composition of the superalloy is Ni-7.8Cr-5.2Co-5Al-2.1Mo-1.5Ti-8W-5.8Ta (wt.%). The loading axis is parallel to the longitudinal [0 0 1] crystallographic direction of the rod. The full heat treatment consisted of a two-step ageing treatment, 6 h at 1080 °C and 20 h at 870 °C in an argon atmosphere, and the typical microstructure of the fully heat-treated single crystal is shown in [Figure 1](#). Samples are mechanically polished with SiC paper, then with diamond paste down to 3  $\mu$ m and cleaned with acetone and alcohol.

Figure 1. Typical microstructure of the single crystal MC2 superalloy.



Creep tests were carried out up to rupture at 1150 °C and 80 MPa under laboratory air. The specimens were heated in a radiation furnace that allows high heating and cooling rates. Two S-type thermocouples were spot-welded: one in the middle of the gauge length to regulate the temperature ( $\pm 2$  °C) and the other one to estimate the thermal gradient. Glass windows let a laser beam go through the furnace and therefore allowed measurement of the relative displacement of two L-shaped flags that were spot-welded on the gauge length (Fig. 2) [3] with an accuracy of 2  $\mu$ m at 1150 °C.

Figure 2. Specimen geometry with location of flags and thermocouples: (a) front view of the tested specimen and location of the laser beam and (b) side view of the assembly [3].



Tensile creep tests were performed under thermal cycling and isothermal conditions. Thermal cycling creep tests were done in the temperature range of 50–1150 °C with heating/cooling rates

fixed at  $5\text{ }^{\circ}\text{C s}^{-1}$  under a constant stress. The load was applied at  $1150\text{ }^{\circ}\text{C}$  at the beginning of the first high-temperature dwell. One cycle corresponds to a heating phase from room temperature to  $1150\text{ }^{\circ}\text{C}$ , followed by isothermal dwell, and controlled cooling to room temperature. An example of the temperature evolution and the associated total strain change to the specimen for two cycles during the thermal cycling creep test is shown in [Figure 3](#).

Figure 3. Creep-test thermal cycles with (a) the temperature profile and (b) the associated total strain change to the specimen.

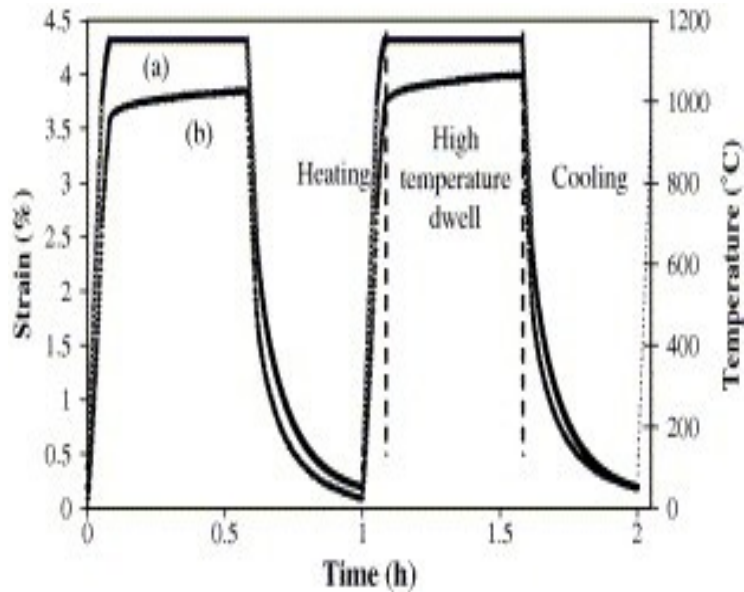


[Figure 4](#) shows the raw continuous strain recording performed during a thermal cycling creep test of the MC2 superalloy. Thermal cycles were repeated until the specimen ruptured. When the sample was heated and cooled, the specimen strain recording varied according to the expansion and contraction of the specimen. Measuring the viscoplastic strain contribution occurring during heating and cooling ramps allows us to ignore this contribution and to plot the global creep strain as the sum of the creep strains that occur during the high-temperature dwells.

Figure 4. Experimental strain change to a MC2 superalloy specimen during a creep test under thermal cycling conditions with dwell at  $1150\text{ }^{\circ}\text{C}$  and constant stress.

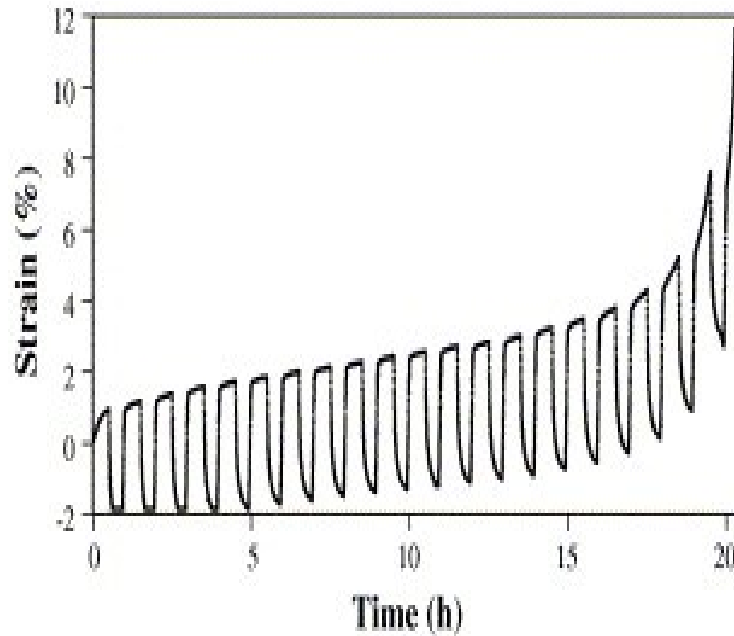
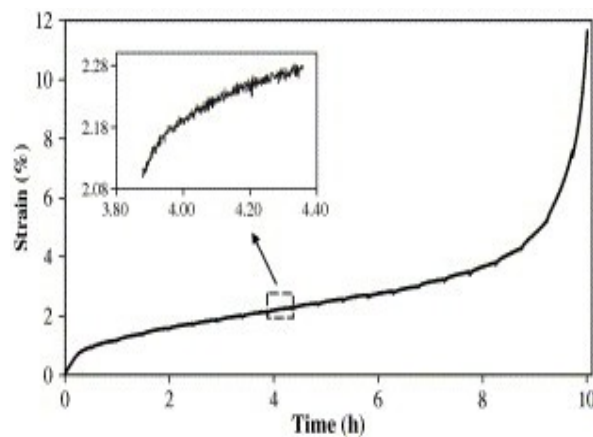


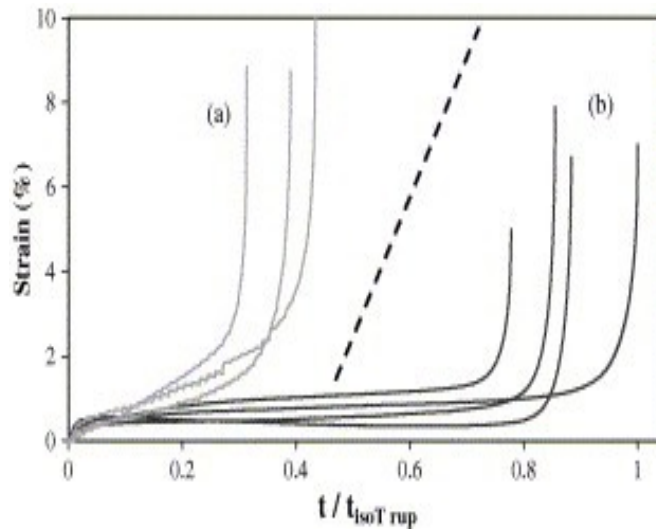
Figure 5 shows the high-temperature strain of a MC2 superalloy sample for a thermal cycling creep test. Strain changes during heating and cooling have been removed, and the resulting curve is the sum of the high-temperature strains. With this procedure, the final curve looks like a typical strain versus time creep curve obtained at high temperature for the single crystal nickel-based MC2 superalloy [4]. The transient strain, produced when the load is applied at the beginning of the first high-temperature dwell, is followed by a longer steady-state stage. Under the applied stress at high temperature,  $\gamma'$  rafting occurs, enhancing the creep resistance [5]. During the steady-state creep stage, the creep strain rate can be measured on the global curve. Thereafter, a tertiary stage of creep occurs just before the specimen rupture.

Figure 5. High-temperature strain of a MC2 superalloy sample during a thermal cycling creep test.



Thermal cycling creep tests have been compared with isothermal creep tests. The different creep curves obtained are shown in Figure 6. Strain is plotted as a function of time/lifetime of the longest isothermal creep test ( $t/t_{\text{isoTrup}}$ ). For high-temperature and low-stress conditions, under isothermal and thermal cycling conditions, superalloys show creep curves with a classical shape divided into three stages: a primary creep (stage I) is followed by a period with nearly constant creep strain rate (stage II). An increase in the strain rate before rupture characterises the last stage (III).

Figure 6. Normalised creep curves of a MC2 superalloy obtained at 1150 °C/80 MPa for (a) thermal cycling creep tests and (b) isothermal creep tests.



A stage of primary creep occurs for the MC2 superalloy as soon as the load is applied. For a given applied stress, the total strain at the end of the primary creep seems to be independent of the type of creep test. The tertiary stage of the thermal cycling and isothermal creep tests are also identical, as far as the strain rate is concerned. Finally, the difference between the two types of creep tests lies essentially in the duration of the steady-state stage, which is responsible of the difference in high-temperature lifetime. A reduction in high-temperature creep life associated with thermal cycling is clearly evidenced. Table 1 shows the lifetime of the creep tests and the comparison with the time to rupture of the longest isothermal creep test performed at 1150 °C/80 MPa. The lifetime of the MC2 superalloy at 1150 °C under thermal cycling creep conditions is at least half that of an isothermal creep test.

Table 1.

Minimum creep rates and times to rupture at 1150 °C and 80 MPa

| Type of creep test | $\dot{\epsilon}$ ( $10^{-4} \text{ h}^{-1}$ ) | $t_{\text{rup}}$ (h) | $\frac{t_{\text{rup}}}{t_{\text{isoTrup}}}$ |
|--------------------|---|----------------------|---|
| Isothermal         | 1.4   | 36.8                 | 1.0   |
| Isothermal         | 2.0   | 28.7                 | 0.8   |

| Type of creep test | $\dot{\epsilon}$ ( $10^{-4} \text{ h}^{-1}$ ) | $t_{\text{rup}}$ (h) | $\frac{t_{\text{rup}}}{t_{\text{isoTrup}}}$ |
|--------------------|---|----------------------|---|
| Isothermal         | — <sup>a</sup>                                | 32.6                 | 0.9   |
| Isothermal         | 1.2   | 31.6                 | 0.9   |
| Thermal cycling    | 23.0  | 11.6                 | 0.3   |
| Thermal cycling    | 13.1  | 14.4                 | 0.4   |
| Thermal cycling    | 9.8   | 16.0                 | 0.4   |

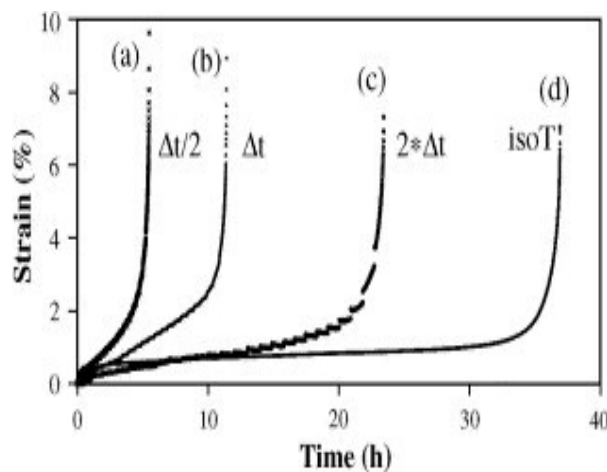
<sup>a</sup> Problem with strain recording.

The minimum creep rate has also been calculated for the different creep tests during the steady-state stage. [Table 1](#) indicates that the minimum creep rate of thermal cycling creep is at least seven times the rate of isothermal creep. The consequence is a decrease in the lifetime to rupture despite an increase in the MC2 superalloy strain to rupture under thermal cycling conditions.

The strain at the onset of the tertiary stage and the strain to rupture are slightly higher under thermal cycling conditions than under isothermal conditions ([Fig. 6](#)). The tertiary stage begins with a critical deformation by about 2% under thermal cycling conditions, and 1% in the case of an isothermal creep test. The recovery of the structure during thermal cycling gives a higher ductility to the superalloy but decreases lifetime at high temperatures, because of the increase in the steady-state creep strain rate.

The effect of the high-temperature dwell time duration, which is equivalent to the effect of the thermal cycle frequency, has also been studied and is shown in [Figure 7](#). Three different types of high-temperature dwell time duration have been chosen ( $\Delta t = 30 \text{ min}$ ;  $\Delta t/2$  and  $2\Delta t$ ).  $\Delta t$  is the dwell time duration previously used to compare thermal cycling and isothermal creep tests ([Fig. 6](#)).

Figure 7. Influence of dwell time duration ( $\Delta t = 30 \text{ min}$ ) on creep lifetime with dwell time duration equal to: (a)  $\Delta t/2$ ; (b)  $\Delta t$ ; (c)  $2 * \Delta t$  and (d) isothermal creep test.



Time to rupture at high temperature increases as the dwell time duration increases, that is, with

decreasing thermal cycle frequency. Increasing the cycle frequency, and therefore repeating the heating and cooling stage during a creep test, is shown to be more damaging to the structure and confirms the deleterious effect of thermal cycling. Conversely, a high-temperature dwell with a long duration improves the superalloy creep resistance.

At temperatures above 950 °C, the dissolution of the  $\gamma'$  precipitates is effective and the volume fraction of  $\gamma'$  decreases as the temperature increases [4]. The succession of heating ( $\gamma'$  dissolution) and cooling ( $\gamma'$  precipitation) affects the stability of the microstructure that controls the steady-state creep rate. This effect is similar to a recovery of the deformation structure, leading to strain transients repeated at each cycle. When zooming in on a cycle (Fig. 5), the strain rate is found to be higher at the beginning of each high-temperature dwell before stabilising. These transient periods lead to a drastic creep rate increase under thermal cycling conditions, and may be linked to a microstructural deterioration caused by the cycle repetition. Directional  $\gamma'$  precipitation and preferential local dissolution under stress may enhance the diffusion process and the coarsening of the rafted  $\gamma/\gamma'$  microstructure, leading to the topological inversion of the phases and to the tertiary creep stage.

Furthermore, damaging kinetics appeared faster under thermal cycling with higher creep rates and shorter dwell times. This observation seems to indicate that the microstructural evolution is accelerated but the morphological change remains the same, as the tertiary stages are identical under the two types of creep tests. Analysing thermal cycling creep fracture shows that the deformation behaviour of the superalloy displays only the creep-like characteristics. The final fracture is preceded by necking and the fracture surface does not show any particular fatigue morphology.

The tests performed under laboratory air have shown the drastic effect of thermal cycling on creep properties of a single crystal nickel-based superalloy at 1150 °C. Thermal cycling during a creep test increases the creep rates and decreases lifetime at high temperature. Furthermore, thermal cycling creep lifetime decreases as the thermal cycle frequency increases.

At temperatures above 950 °C, the dissolution of the coherent  $\gamma'$  precipitates and their subsequent reprecipitation on cooling affect the mechanical behaviour of the alloy and the creep lifetime. The analysis of the microstructure and the stability of the dislocation networks at the  $\gamma/\gamma'$  interface is in progress in order to understand the micromechanisms involved.

The above results confirm the necessity of performing tests with more complex thermomechanical loading closer to the in-service situation of blades. This will allow a better modelling of the stress rupture of a single crystal nickel-based superalloy.

## **References**

P. Caron and T. Khan, *Aerosp. Sci. Technol.* **3** (1999), p. 513.

P. Caron and T. Khan In: H.E. Exner and V. Schumacher, Editors, *Advanced materials and processes, Advanced Processing and High Temperature Materials*, DGM Informationgesellschaft mbH, Oberursel (1990), pp. 333–338.

S. Dryepondt, D. Monceau, F. Crabos and A. Andrieu, *Acta Mater.* **53** (2005), p. 4199.

P. Caron In: T.M. Pollock *et al.*, Editors, *Superalloys 2000*, TMS The Minerals, Metals and Materials Society, Warrendale, PA (2000), pp. 737–745.

A. Epishin and T. Link In: K.A. Green *et al.*, Editors, *Superalloys 2004*, TMS The Minerals, Metals and Materials Society, Warrendale, PA (2004), pp. 137–143.



Corresponding author. Tel.: +33 562885710; fax: +33 562885663.

**Original text : [Elsevier.com](http://Elsevier.com)**